

## EFFECT OF HIGH-PASS CUT-OFF FREQUENCY ON STRUCTURAL RESPONSE UNDER THE STRONG GROUND MOTION

Fatma Sevil MALCIOGLU<sup>1</sup> & Tugce TETIK<sup>2</sup>

**Abstract:** *A great variety of external sources such as wind, ambient noise, instrumental effects, etc. is responsible for the contamination of strong ground motion (SGM). That's why, the recorded raw acceleration time series include noise signal, as well as actual earthquake motion. Removal of these noises from acceleration series is the primary stage of data processing in earthquake engineering applications because of the frequency dependence of structural response. When considered the long period structures, elimination of especially low-frequency noises in SGM gains considerable importance. From this consideration, low-frequency noise in the data and hence structural response vary depending on the selection of low cut-off in the data processing. This study aims to investigate the effect of high-pass cut-offs ( $f_{hp}$ ) on peak SGM parameters and structural response of the equivalent single degree of freedom systems (SDOFs). For that purpose, linear and nonlinear dynamic analyses of the systems were performed by BISPEC Professional computer program and computed constant-ductility spectra ( $C_{\mu}$ ) and constant-strength spectra ( $C_R$ ) to identify the effect of selection of  $f_{hp}$  on structural response. Peak ground acceleration (PGA),  $C_R$  and  $C_{\mu}$  are affected by the choice of high-pass cut-offs. However, the extent of the variation is primarily governed by the magnitude, soil conditions and structural period range of interest as well. Especially, PGAs of large events and from soft soils are most susceptible to variation of  $f_{hp}$ . As for spectral displacements, the most reliable range for  $f_{hp}$  may be acceptable up to 0.2 Hz in the elastic analysis. Additionally, higher inelasticity produces a greater effect on  $C_R$  &  $C_{\mu}$ .*

### Introduction

The low and high frequency noises may be responsible for the physically unjustifiable frequency content in high and low frequency component of ground motion (Akkar et al., (2014)). Processing of strong ground motion records is a crucial procedure to decontaminate the frequency content, hence, obtain reliable data for earthquake engineering purposes. Tendo et al. (1992) in Douglas (2003) emphasizes the critical importance of data correction procedures in the derivation of ground motion prediction equations (GMPE) which estimate ground motion parameters such as peak ground values and response spectral ordinates and possible inhomogeneities and errors due to the subjectivity in the selection of filter corners. In the study of Bazzurro et al. (2004), effects of processing techniques on elastic and inelastic spectra are noticed especially for long period region. Furthermore, Akkar and Bommer (2006) point out the substantial role of a reliably processed ground motion dataset in displacement based design and seismic performance assessment procedures. Also, in the same study, it is remarked the necessity of especially low frequency noise elimination from strong ground motion data since structural performance are modelled in terms of seismic displacement demands. In this context, high-pass filtering is an inevitable part of the data processing of the strong ground motion to subtract the low frequency (long period) noise (Boore et al. (2012)).

Since various values of high-pass cut-off frequency ( $f_{hp}$ ) may lead to considerably different values of peak ground motion parameters and spectral amplitudes, the identification of the extent to which high-pass filtering influences these parameters may shed light into the selection of high-pass cut-off frequencies in the data processing stage. For that purpose, the first part of this study compares the peak values of accelerations, velocities, and displacements for detrended and high-

---

<sup>1</sup> Research Assistant, Bogazici University, Kandilli Observatory & Earthquake Research Institute, Istanbul, Turkey, sevil.malcioглу@boun.edu.tr

<sup>2</sup> Research Assistant, Bogazici University, Kandilli Observatory & Earthquake Research Institute, Istanbul, Turkey

pass filtered data. Elastic and inelastic analyses of SDOF systems under detrended and filtered ground motions and their comparisons constitute the second stage of the study to identify the effect of high-pass cut-offs on these parameters.

## Characteristics of ground motion database

### Selection of earthquakes

The official strong motion database of the Republic of Turkey Prime Ministry Disaster & Emergency Management Authority (DEMA) was investigated for the selection of earthquakes and strong ground motion records. Latest earthquakes were preferred except for Central Kocaeli (17/08/1999) event owing to an increase in the number of strong ground motion records thanks to the enhancement of the Turkish National Strong Motion Network in recent years. A dataset consisting of 11 earthquakes from Turkey regardless of faulting types was generated. The first criterion for the selection of earthquakes is based upon representation of all magnitude ranges larger than 4.0 to identify the effect of high-pass filtering associated with the magnitude. For that purpose, earthquakes were classified as 4 groups with respect to moment magnitudes ( $M_w$ ) ranging from 4.1 to 7.6 as seen in Table 1.












Classification based on $M_w$	Date	Epicentre	Moment Magnitude ( $M_w$ )	Depth (km)	Focal Mechanism
Group 1	30/11/2018	Yalova/Cinarcik	4.1	14.28	
	20/12/2018	Yalova/Cinarcik	4.5	12.47	
Group 2	07/04/2018	Central Bolu	4.7	10.47	
	28/05/2017	Manisa/Saruhanli	4.8	6.90	
	27/05/2017	Manisa/Saruhanli	5.1	11.03	
Group 3	02/03/2017	Adiyaman/Samsat	5.5	9.76	
	16/04/2015	The Mediterranean Sea/ Eastern Basin	5.9	12.34	
	12/06/2017	Aegean Sea	6.2	15.86	
Group 4	20/07/2017	Off the coast of Bodrum	6.5	19.44	
	23/10/2011	Central Van	7.0	19.02	
	17/08/1999	Central Kocaeli	7.6	17.00	

Table 1. Main characteristics of earthquakes compiled from DEMAs (\*the focal mechanism is taken from USGS, others are compiled from KOERI website).

### Selection of strong ground motion records

All raw acceleration traces of the previously mentioned earthquakes were compiled from the stations within Turkey. The rejection criterion for stations is primarily based on average shear wave velocity for the upper 30 m depth ( $V_{s,30}$ ). Stations with no  $V_{s,30}$  information and including only one horizontal component were discarded in this study. Furthermore, to recognize explicitly the effect of the site condition, records were classified two site categories based on the values of  $V_{s,30}$  and records from stations with  $350 < V_{s,30} < 600$  m/sec were not incorporated in the analyses to draw precisely the distinction between two soil group. While acceleration time histories recorded at stations with  $V_{s,30} < 350$  m/sec was accepted as soft soil records, those with  $V_{s,30} > 600$  m/sec

were assumed as stiff soil stations relatively. In the whole dataset, the station  $V_{s,30}$  value ranges from 131 m/sec to 1380 m/sec. So, with the addition of soil site classification, the number of groups enhanced from 4 to 8.

As a result of the rejection criteria, the total dataset comprises 510 acceleration traces when including both horizontal components (NS and EW) from 107 stations. The distribution of  $V_{s,30}$  values for each magnitude class is illustrated in Figure 1. Within each magnitude interval, the average values of  $V_{s,30}$  for each soil type correspond to identical values. As for the number of data for each group, stiff soils always suffer from a lack of data when compared to soft soils.

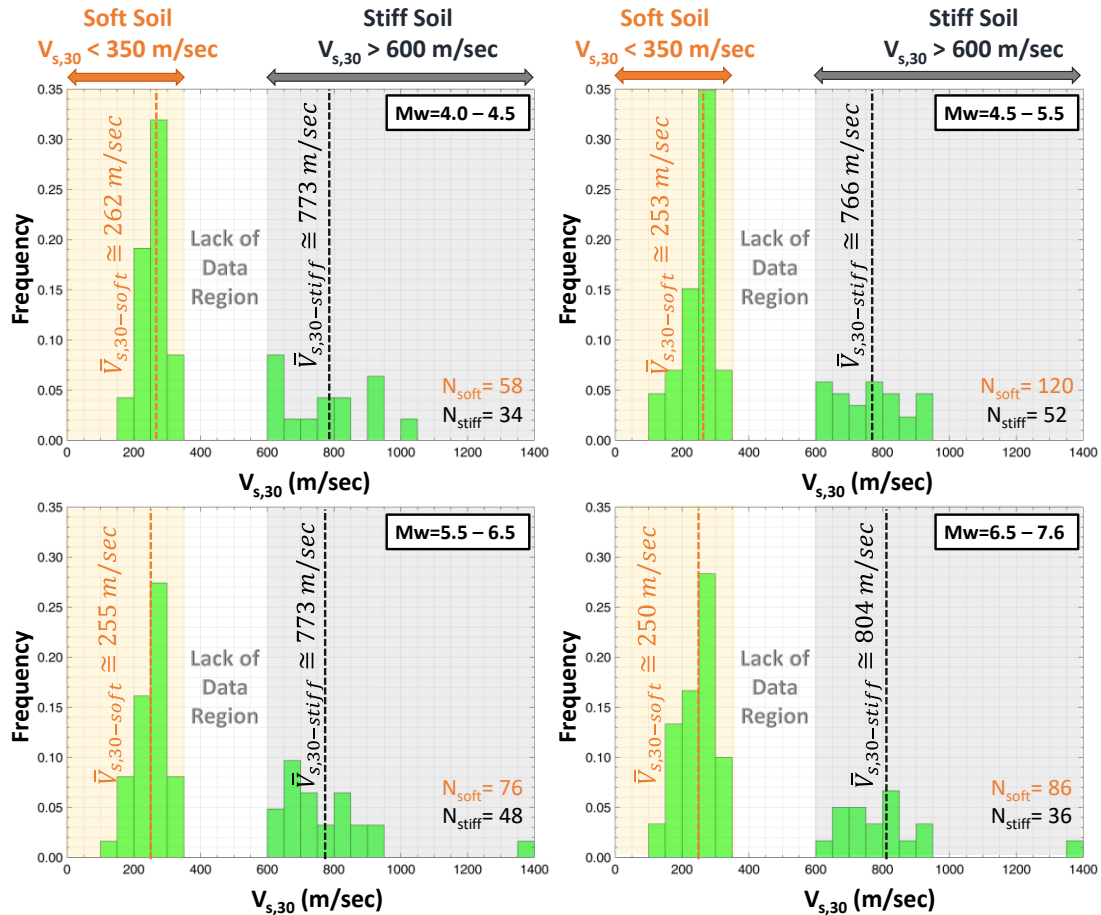


Figure 1. Distribution of average shear wave velocities of stations for the upper 30 m depth ( $V_{s,30}$ ) ( $\bar{V}_{s,30}$  and  $N$  corresponds to mean  $V_{s,30}$  value and number of data for each group, respectively).

### Data processing scheme

#### Baseline corrections

When numerical integration is applied to recorded raw acceleration signals, the baseline shifts on velocity and displacement traces are mostly detected due to inconsistency between assumed and real values of initial velocity and displacements. In order to cope with this issue, the most commonly used algorithm is based upon the removal of the polynomial trend from an acceleration time history (Pan et al. 2016).

In order to provide physically meaningful velocities and displacements, the detrending algorithm was performed on all raw acceleration time histories by subtracting the mean of whole time series via Matlab. In this study, these accelerations are called as ‘detrended acceleration ( $A_d$ )’.

#### Filtering

High-pass filtering is mostly applied to acceleration records in order to eliminate the low frequency (long period) noise contamination. In the data processing stage, the accurate determination of

high-pass cut-off frequency is a prominent step to obtain more reliable data for further analysis. In consideration of these, each acceleration traces were exposed to high-pass filtering for different high-pass cut-off frequencies ranging from 0.02 Hz to 1 Hz with an interval of 0.001 Hz. Therefore, 981 filtered data was derived for each acceleration time histories. When considered the number of accelerations, 510 traces, the total number of generated time histories including detrended accelerations equals to 500.820.

In order to perform high-pass filtering, Butterworth filter (4<sup>th</sup> order), the most widely used filter type in data processing of strong ground motions, was applied to these acceleration traces. The frequency response function of the Butterworth filter is analytically described as follows,

$$|H_{\omega}| = \frac{1}{\sqrt{1 + \left(\frac{\omega}{\omega_c}\right)^{2n}}} \quad (1)$$

In which,  $\omega$  is the generic angular frequency,  $\omega_c$  represents the cut-off frequency, and  $n$  is the filter order (Cimellaro and Marasco, 2015).

### Influence of high-pass cut-off on ground motion parameters

The initial evaluation of the high-pass cut-off effect is conducted for peak ground motion parameters (PGA, PGV, PGD, and peak Fourier amplitudes (PFAS)) in this section. Moreover, the time and frequencies corresponding to peak values are also examined herein.

The velocities and displacements were computed by the integration of all detrended and filtered acceleration traces for each magnitude and soil group. In order to pinpoint explicitly the extent to which detrended data has changed when high-pass filtering was applied, the ratios of peak values of filtered data to those of detrended time series were calculated and then the arithmetic means of ratios were taken for each high-pass cut-off value.

Figure 2 illustrates the variation of the mean ratios with the increasing values of high-pass cut-off frequencies for each subgroup categorized according to magnitude and  $V_{s,30}$  of station sites. In the figure, stiff soils ( $V_{s,30} > 600$  m/sec) are designated as grey lines while coloured lines represent the soft soil ( $V_{s,30} < 350$  m/sec).

The influence of high-pass cut-off frequencies are more apparent in the PGA and say, PFAS. As expected, the increase in high-pass cut-offs is responsible for the reduction in PGA and PFAS values. However, when compared results of detrended and filtered data for small magnitude events ( $4.0 < M_w < 4.5$ ), there exist no noticeable variation within the  $f_{hp}$  range of concern. As for larger magnitudes, the impact of low frequency content elimination becomes more evident. Regarding soil effect, soft soil is more sensitive to the variation of high-pass cutoffs in terms of PGA. However, in the largest magnitude range ( $6.5 < M_w < 7.6$ ), the influence of soil condition cannot be noticed apparently. This may be attributed to peak acceleration values at lower frequencies detected in several stiff-soil records when examined Fourier amplitude spectrums of each record in detail.

The mean ratio of PGVs exhibits a decreasing trend with the removal of low frequency data especially for greater magnitudes ( $5.5 < M_w < 6.5$  &  $6.5 < M_w < 7.6$ ). For smaller magnitudes, despite of a slightly decreasing trend, the general tendency can be assumed as approximately stable for different values of  $f_{hp}$ . PGV ratio increases with the decrement of magnitudes for soft soils, however, vice versa for stiff soils except for largest magnitude class. For soft soil data within the intermediate range of magnitudes ( $4.5 < M_w < 5.5$ ), mean PGV ratios approaches to 1.0. In other words, PGV in the intermediate ranges of magnitudes is less affected by the filtering process herein.

As to PGD ratios, as expected, when filtered the data with higher  $f_{hp}$ , the deviation of PGD values from detrended one is remarkably noticeable. For the initial value of  $f_{hp}$ , 0.02 Hz,  $PGD_{fd}/PGD_d$  ratios take the value of larger than 1.0 for all groups, then, the variation of ratios exhibits almost linear decay in logarithmic scale. However, the variation of mean PGD ratios with magnitudes and soil types cannot reveal reliable information.

The right column of Figure 2 also shows the changes in times and frequency at which the detrended and high-pass filtered data reach their absolute peak values. For lower magnitudes than 6.5, the variation in time corresponding to PGA may be negligible. However, ascending

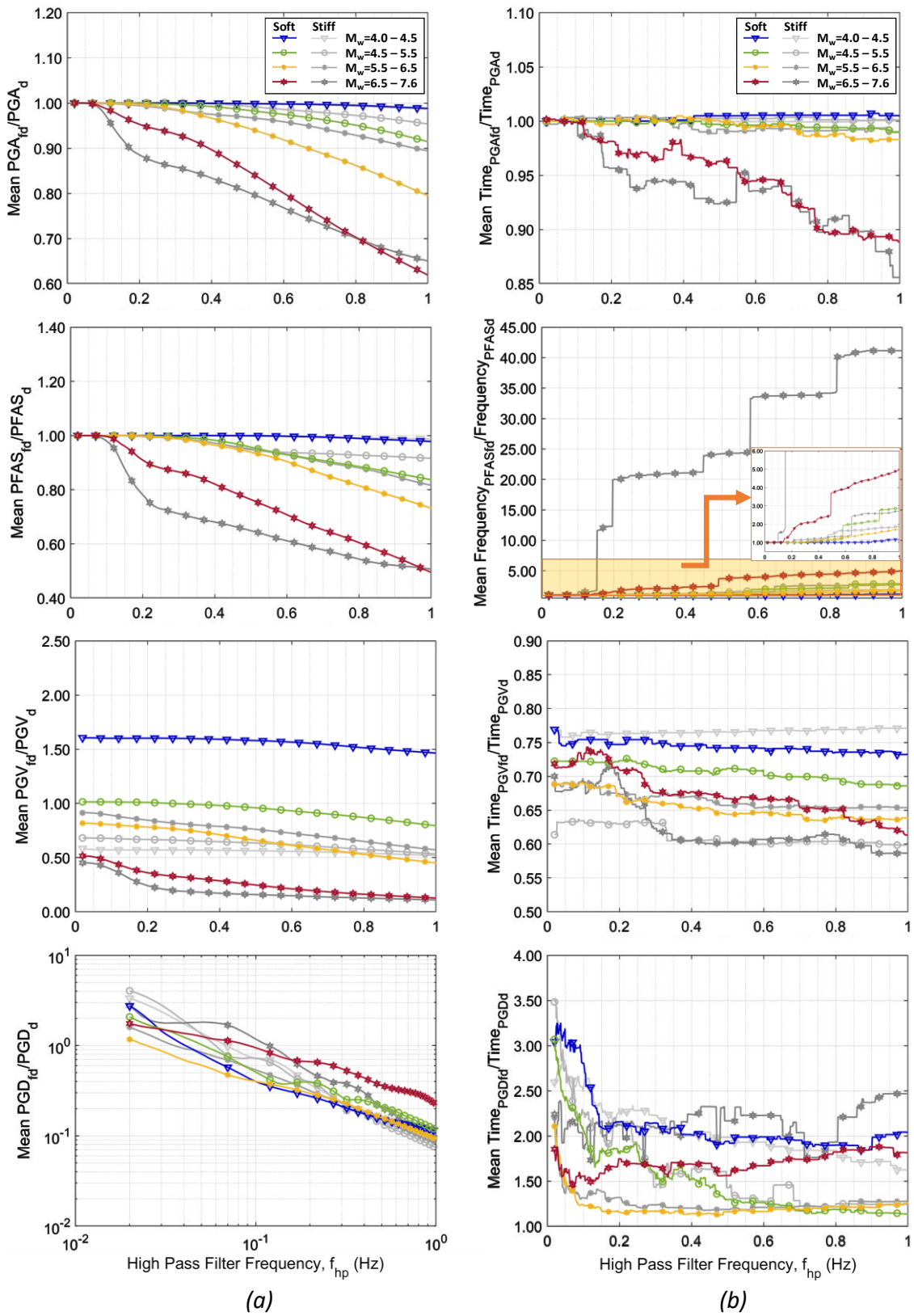


Figure 2. Variation of mean ratios -filtered to detrended data- of (a) peak ground motion parameters (acceleration, velocity, displacement and Fourier amplitudes), (b) times and frequency corresponding to peak values.

values of  $f_{hp}$  give rise to the significantly early generation of peaks within the magnitude range between 6.5-7.6. Frequencies at which the peak Fourier amplitudes occur move to higher frequencies with the elimination of low frequency content. While this movement begins at the smaller  $f_{hp}$  values for the larger magnitudes, with the decrease in magnitudes, the ratio of frequencies corresponding to PFAS start to fall down at the higher  $f_{hp}$  values. As for the occurrence time of PGV, for all magnitudes and soil types, peak values of filtered data occurs earlier than those of detrended data. When examined increasing values of  $f_{hp}$ , they exhibit an almost constant trend except for the largest magnitude range. For  $6.5 < M_w < 7.6$  class, the ratio tends to decrease with the elimination of low frequency content. In contrast to PGV, occurrence times of PGDs are shifted to further, however, a stable trend with  $f_{hp}$  is similar after a rapid decrease.

### Influence of high-pass cut-off on elastic and inelastic displacements

#### The theoretical basis of the elastic and inelastic dynamic analysis

For SDOFs, the main philosophy of the elastic and inelastic analysis is based on the solution of the equation of motion under the lateral forces arisen from earthquake ground motions. When assumed that the force-deformation relation of SDOFs displays linearly elastic behaviour, the equation of motion are solved for elastic forces,  $f_0$  corresponding to elastic deformation,  $u_0$ . However, these elastic forces are usually very large and laboratory experiments indicate that force-deformation behaviour of structures for earthquake conditions exhibits cyclic characteristics (hysteresis relations) (Chopra (2001)).

In this study, both elastic and inelastic analyses were conducted under the detrended and filtered ground motions. For inelastic nonlinear analysis, force-deformation relation was assumed as to be consistent with Clough stiffness degrading model (Figure 3) representing reinforced concrete structures. In this model, when cyclic lateral loads become reversal, stiffness of the system degrades.

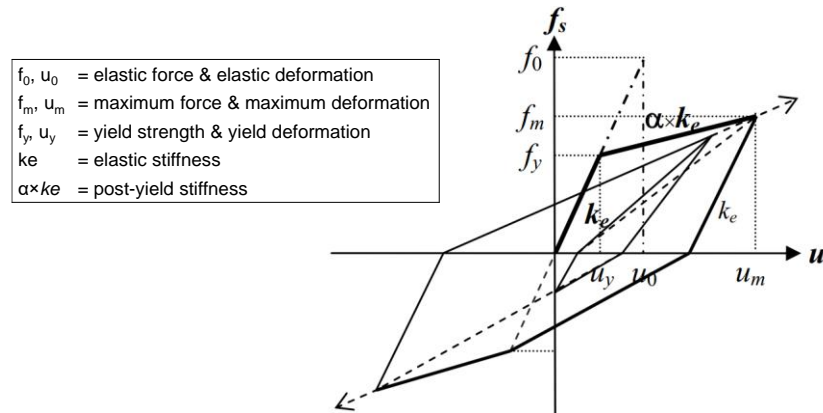


Figure 3. Hysteretic model (Clough stiffness degradation) used in the analysis (Modified from Malcioglu and Taskin, 2013).

The inelastic deformation ratio ( $C_\mu$  and  $C_R$ ) is a useful tool to obtain the inelastic deformation of a new or existing structures. Using hysteresis force-deformation relation as seen in Figure 3, ductility factor ( $\mu$ ), strength reduction factor ( $R$ ) and the ratio of peak deformation,  $u_m$  to  $u_0$  can be established as following;

$$\mu = \frac{u_m}{u_y} ; R = \frac{f_0}{f_y} = \frac{u_0}{u_y} \rightarrow \frac{\mu}{R} = \frac{u_m}{u_0} \quad (2)$$

The needed parameters,  $u_m$  and  $u_0$ , to determine  $\mu/R$  ratio can easily be calculated by the numerical solution of the dynamic equation of motion for the inelastic force deformation relation and its corresponding linear SDOF system. As defined by Chopra (2001), the inelastic deformation ratios for the existing structures with known yield strength ( $C_R$ ) or for the new structures with known ductility ( $C_\mu$ ) are determined by Equation (3).

$$C_R = \frac{u_m}{u_0} \quad \text{or} \quad C_\mu = \frac{u_m}{u_0} \quad (3)$$

### *Evaluation of elastic responses under high-pass filtered ground motions*

The elastic analyses were performed in Matlab via Newmark linear method approximation under detrended and filtered ground motions for SDOFs with 5% damping ratio whose periods are ranging from 0 to 4.0 sec. Similar to the evaluation of peak ground motion parameters, the average ratios of filtered spectral displacements to detrended ones ( $S_{df}/S_{dd}$ ) were computed to interpret the effect of  $f_{hp}$  on spectral displacements.

In order to examine the variation of the ratio with both periods of SDOFs and  $f_{hp}$ ,  $S_{df}/S_{dd}$  is illustrated by 2D contour plots as seen in Figure 4. The variation of  $S_{df}/S_{dd}$  for all groups expresses the similar tendency. Spectral displacements from the data filtered up to almost 0.2 Hz gives identical results for all periods of SDOFs when compared to those of detrended data. Except for the largest magnitude group, for SDOFs with up to the period of approximately 0.5 sec, spectral displacements are independent of  $f_{hp}$ . However, in general, the decrement of  $S_{df}/S_{dd}$  ratio strictly depends on the relation between the period of SDOFs and  $f_{hp}$ . The initiation of decay corresponds to periods lower than  $1/f_{hp}$ . Since the aim of high pass filtering is the elimination of low frequency content, major alterations are prominently seen in the long period region. As for effects of site conditions, spectral displacements calculated from stiff soil records are mostly influenced by the variation of  $f_{hp}$ , especially in the long period region. Moreover, when evaluated based on magnitude classes, the greater the magnitude, the more affected the ratio of  $S_{df}/S_{dd}$ .

### *Evaluation of inelastic responses under high-pass filtered ground motions*

In order to obtain inelastic responses, nonlinear dynamic analyses were performed in BISPEC Professional computer program (2012) for SDOFs with 5% damping ratio and unit mass under the detrended and filtered ground motions. It should be noted that the analyses were conducted for only Group 3 ( $5.5 < M_w < 6.5$ ) dataset for both soft and stiff soils. The periods of the systems are ranging from 0.05 to 5 sec. In the analysis, the post-yield strength,  $\alpha$  and the ratio of positive to negative loading were reckoned as 10% and 1.0, respectively. Two sets of computations were conducted for constant  $R$  and constant  $\mu$  ( $R \& \mu = 2; 8$ ) systems to obtain mean inelastic deformation ratios (mean  $C_R$  and  $C_\mu$ ). These ratios are depicted as  $C_{dR}$  &  $C_{d\mu}$  for detrended data and  $C_{fR}$  &  $C_{f\mu}$  for filtered data. Then,  $C_{fR}$  &  $C_{f\mu}$  were normalized to  $C_{dR}$  &  $C_{d\mu}$  to recognize the effect of the filtering process.

Figure 5 demonstrates the effect of  $f_{hp}$  on mean inelastic deformation ratios. The variation of  $f_{hp}$  is highly influential in the mean  $C_R$  and  $C_\mu$  of the systems belonging to higher inelasticity. In other words, the effect of  $f_{hp}$  on inelastic deformation demands is more apparent in the weaker systems. In the general trend, the normalized mean inelastic deformation ratios first decrease with increasing values of the period. Then,  $C_{fR}/C_{dR}$  begins to increase and reaches a minimum ratio at the periods lower than  $1/f_{hp}$ . Finally, it enhances and exceeds the value of 1.0 in the long period region. All aforementioned cycle can be observed for the  $f_{hp} \geq 0.4$  Hz within the period range of interest (0-4 sec) in Figure 5. As expected, the systems exposed to ground motions filtered with higher  $f_{hp}$  are most affected by the filtering process. The deviations of  $C_{fR}$  from  $C_{dR}$  become larger and begin to occur at the lower periods with the increase in  $f_{hp}$ . The effects of soil conditions are more explicit for the systems subjected to the strong ground motions filtered below 0.6 Hz and inelastic deformation ratios computed from filtered soft soil ground motions are closer to  $C_{dR}$  than those of stiff soils.

Similar calculations are performed for systems with selected ductility constant levels of  $\mu=2$  and 8. The variation and comparison of normalized mean inelastic deformation ratios verify the above results of  $C_R$  computations.

## **Conclusion**

The peak ground motion parameters and elastic & inelastic spectral displacements are sensitive to the choice of high-pass cut-off frequencies; however, it depends on the earthquake magnitude and soil types. In other words, when applied high-pass filtering to ground motions, the magnitudes of earthquakes and soil conditions of the recorded site should be taken into account on a record-by-record basis.

This paper indicates that PGA values of acceleration traces for magnitudes less than 4.5 are usually unaffected by the high-pass cut-offs smaller than 1 Hz. However, for larger magnitudes, it exhibits a decreasing trend similar to PGV and PGD. There are no exact inferences for the effect of  $f_{hp}$  on PGV and PGD values in terms of magnitude and site conditions in this study.

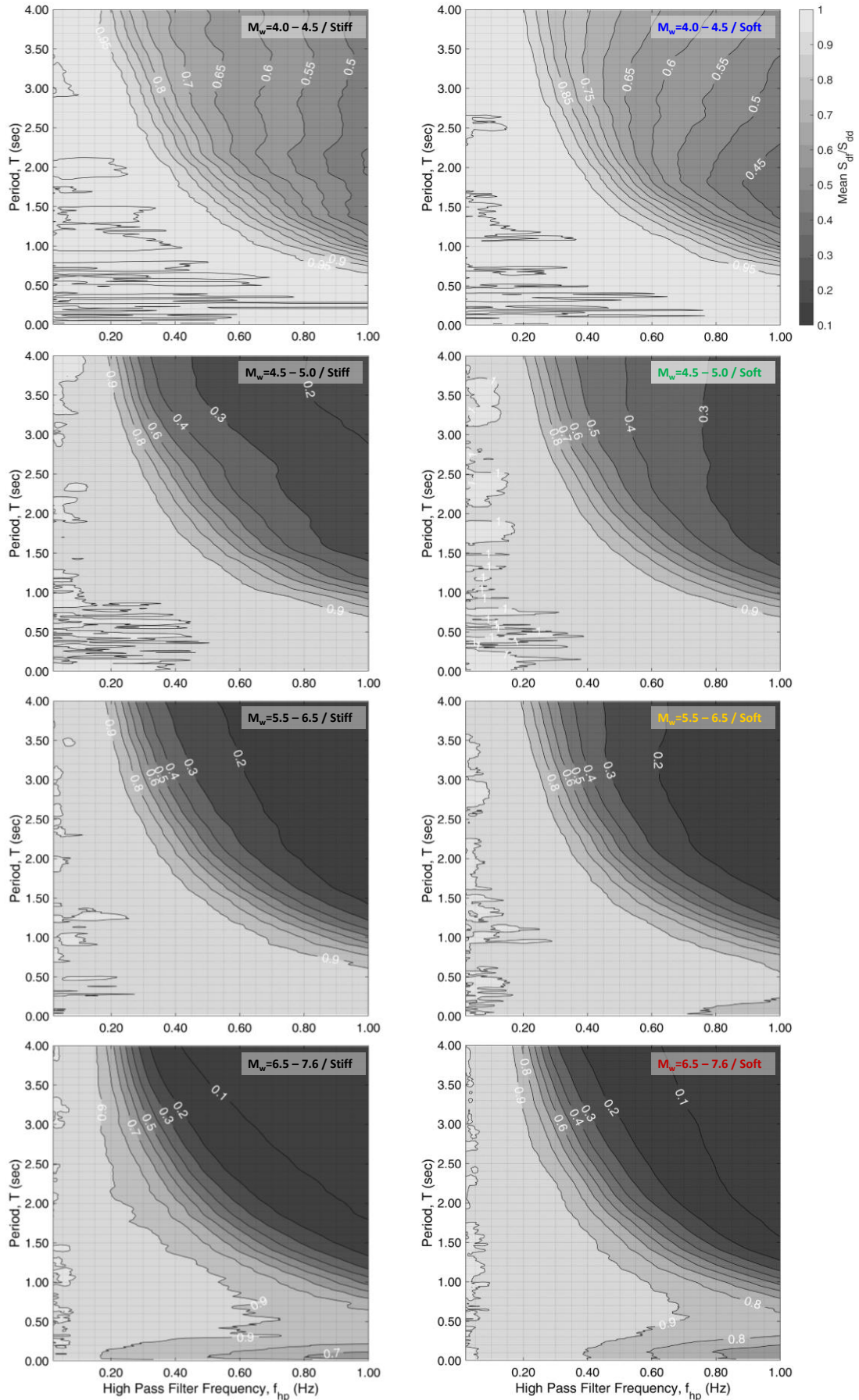


Figure 4. Variation of mean ratios -filtered to detrended- of elastic spectral displacements ( $S_{df}/S_{dd}$ ).



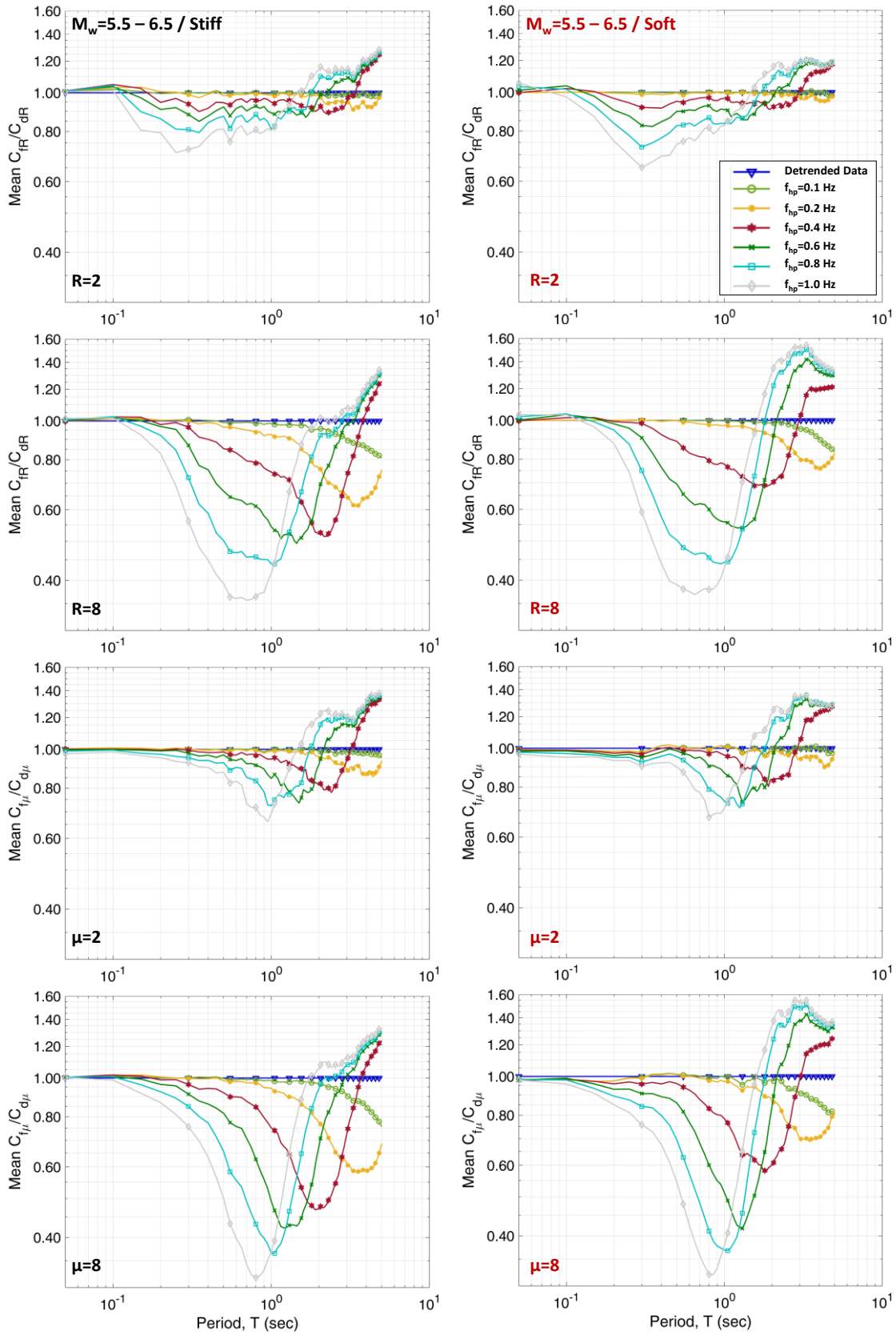


Figure 5. Variation of normalized -filtered to detrended- mean inelastic deformation ratios,  $C_{fR}/C_{dR}$  and  $C_{f\mu}/C_{d\mu}$  for constant  $R$  and  $\mu$  values (2 and 8) of Clough stiffness degradation model.

Moreover, occurrence time and frequencies of PGA and PFAS are influenced by the high-pass cut-offs. While occurrence times of peak values remain approximately constant for different  $f_{hp}$  values, frequencies move to further with the increasing values of  $f_{hp}$ .

As for results of elastic spectral analyses, spectral displacements of SDOFs may be affected by the high-pass cut-offs with the variation of earthquake magnitudes and soil conditions. An unaffected region can be defined based on the period of SDOFs and high-pass cut-off frequencies. Outside of this region, the general trend tends to deviate of mean spectral displacements calculated by filtered data from those of detrended ones. Especially, in the long period region, elastic spectral displacements exhibit mostly decreasing behaviour.

The four times increment in inelasticity indicates that  $R$  and  $\mu$  are the boosting factors for  $f_{hp}$  effects on inelastic deformation demand. Furthermore, the increase in  $f_{hp}$  is responsible for the initiation of the deviation from inelastic deformation ratios belonging to detrended data and arrival to minimum ratios at lower periods.

All these analyses may be repeated for more comprehensive data processing scheme by considering the effect of filter order, the causality of filtering, zero paddings, etc. Especially, the large magnitude issue in this study still needs to be addressed in the future works to accurately obtain the effect of high-pass cut-off frequencies.

## References

- Akkar S and Bommer JJ (2006), Influence of long-period filter cut-off on elastic spectral displacements, *Earthquake Engineering and Structural Dynamics*, 35:1145–1165.
- Akkar S, Sandikkaya MA, Senyurt M, Azari Sisi A, Ay BÖ, Traversa P, Douglas J, Cotton F, Luzi L, Hernandez B and Godey S (2014), Reference database for seismic ground-motion in Europe (RESORCE), *Bulletin of Earthquake Engineering*, 12:311–339.
- Bazzurro P, Sjöberg B, Luco N, Silva W and Darragh R (2004), Effects of strong motion processing procedures on time histories, elastic and inelastic spectra, Invited Workshop on Strong Motion Record Processing, *Consortium of Organizations for Strong-Motion Observation Systems (COSMOS)*, Richmond, CA.
- BISPEC Professional V:2.18 (2012), Earthquake Solutions Inc., CA, USA.
- Boore D, Azari Sisi A and Akkar S (2014), Using Pad-Stripped Acausally Filtered Strong-Motion Data, *Bulletin of the Seismological Society of America*, 102(2): 751–760.
- Chopra AK (2001), *Dynamics of Structures: Theory and Applications to Earthquake Engineering*, Prentice-Hall Inc., NJ, USA.
- Cimellaro GP and Marasco S (2015), A computer-based environment for processing and selection of seismic ground motion records: Opensignal, *Journal Frontiers in Built Environment*, 1(17): 1-13.
- Douglas, J (2003), Earthquake ground motion estimation using strong-motion records: a review of equations for the estimation of peak ground acceleration and response spectral ordinates, *Earth-Science Reviews*, 61: 43–104.
- Malcioğlu FS and Taskin B, *Investigation of the Effect of Noise Content in the Recorded Strong Motions in Structural Behavior*, The 2011 International Conference on Earthquakes and Structures, Seoul, Korea.
- Pan C, Zhang R, Luo H and Hua S (2016), Baseline correction of vibration acceleration signals with inconsistent initial velocity and displacement, *Advances in Mechanical Engineering*, 8(10): 1-11.
- DEMA (2019). Republic of Turkey Prime Ministry Disaster & Emergency Management Authority (DEMA) Official Website. Available at: <http://kyhdata.deprem.gov.tr> (Accessed 05/03/2019)
- KOERI (2019). Bogazici University Kandilli Observatory and Earthquake Research Institute (KOERI) Official Website. Available at: <http://www.koeri.boun.edu.tr/sismo/2/moment-tensor-solutions/> (Accessed 22/04/2019)
- USGS (2019). United States Geological Survey (USGS) Official Website. Available at: Management Authority Official Website. Available at: <https://earthquake.usgs.gov/earthquakes/eventpage/usp0009d4z/focal-mechanism> (Accessed 22/04/2019)